Journal of ELECTRONIC MATERIALS, Vol. 43, No. 7, 2014
DOI: 10.1007/s11664-014-3103-8

Thermoelectric Properties of Magnesium Silicide Deposited by Use of an Atmospheric Plasma Thermal Spray

GAOSHENG FU,[1] LEI ZUO,[1,3] JON LONGTIN,[1] CHAO NIE,[1] YIKAI CHEN,[2] MAHDER TEWOLDE,[1] and SANJAY SAMPATH[2]

1.—Department of Mechanical Engineering, State University of New York at Stony Brook, Stony Brook, NY 11794, USA. 2.—Department of Material Science and Engineering, State University of New York at Stony Brook, Stony Brook, NY 11794, USA. 3.—e-mail: lei.zuo@stonybrook.edu

The thermoelectric properties of magnesium silicide (Mg_2Si) samples prepared by use of an atmospheric plasma spray (APS) were compared with those of samples prepared from the same feedstock powder by use of the conventional hot-pressing method. The characterization performed included measurement of thermal conductivity, electrical conductivity, Seebeck coefficient, and figure of merit, *ZT*. X-ray diffraction (XRD), scanning electron microscopy (SEM), and energy dispersive x-ray spectroscopy (EDX) were used to assess how phase and microstructure affected the thermoelectric properties of the samples. Hall effect measurements furnished carrier concentration, and measurement of Hall mobility provided further insight into electrical conductivity and Seebeck coefficient. Low temperature and high velocity APS using an internal-powder distribution system achieved a phase of composition similar to that of the feedstock powder. Thermal spraying was demonstrated in this work to be an effective means of reducing the thermal conductivity of Mg_2Si; this may be because of pores and cracks in the sprayed sample. Vacuum-annealed APS samples were found to have very high Seebeck coefficients. To further improve the figure of merit, carrier concentration must be adjusted and carrier mobility must be enhanced.

Key words: Thermoelectrics, magnesium silicide, thermal spray, APS, figure of merit

INTRODUCTION

Energy use for vehicle transport is a large fraction of domestic energy use.[1] In these applications, more than one third of the energy is wasted as engine exhaust.[2] Although the engine thermodynamics necessitate this heat discharge, it can be recovered and used for production of electricity. Examples of this approach include organic Rankine cycles,[3] mechanical turbochargers,[4] electric turbochargers,[5] and thermoelectric generators (TEGs). In all of these applications, the objective is to increase fuel efficiency. As a solid-state energy-conversion device, TEGs have many benefits for converting automobile engine exhaust into electrical power. Recent research supported by the US Department of Energy indicated that 350–390 W of electricity recovery can increase fuel efficiency by 3% for a mid-size truck and 4% for a sedan.[6]

The conversion efficiency of a thermoelectric material is determined by its figure of merit *ZT*:[7]

$$ZT = \sigma S^2 T/k, \tag{1}$$

where S is the Seebeck coefficient (V/K), σ is the electrical conductivity (S/m), κ is the thermal conductivity (W/m K), and T is the absolute temperature in Kelvin (K). The electrical conductivity $\sigma = ne\mu$ is given by carrier concentration n, carrier mobility μ, and electron charge e. Carrier concentration and mobility can be characterized by measuring the Hall coefficient R_H. For materials in which electrons are the main carriers, $R_H = -1/ne$.

(Received April 8, 2013; accepted March 3, 2014; published online April 1, 2014)

Combining the Hall effect coefficient and electrical conductivity, $\mu = -\sigma R_H$. The Seebeek coefficient is defined in several different ways depending on the situation. A common definition from Busch and Winkler for n-type thermoelectric material is:[8]

$$S = -\frac{k}{e}\left(\frac{5}{2} + r + \ln\frac{N_c}{n}\right). \quad (2)$$

Here k is Boltzmann constant, r is an exponent of the power function in the energy-dependent relaxation time expression, and N_c is the effective density of states in the valence band. It is apparent the Seebeck coefficient is affected by carrier concentration, n.

Materials that have a large Seebeck coefficient, large electrical conductivity, and low thermal conductivity have large values of ZT and thus are attractive for thermoelectric applications. However, the underlying conditions can affect these properties in opposite ways. For example S and σ have an opposing dependence on n, with the result that the optimum ZT will lie in the mid-range of carrier concentration.

Extensive interest and research over the past decade continues to investigate new potential thermoelectric materials. Among these, Mg_2Si is of particular interest in applications for recovery of automobile exhaust heat,[9,10] because it has reasonable ZT in the exhaust temperature range and Mg and Si are abundant on earth, thus making it much less expensive than traditional thermoelectric materials, for example bismuth telluride.

Some progress has been reported on the synthesis of Mg_2Si and its solid solutions. Zaitsev et al.[11] investigated Mg_2Si–Mg_2Sn solid solutions and achieved a maximum ZT of 1.1. Isoda et al.[12] developed a liquid–solid reaction followed by hot pressing and obtained a maximum ZT of 1.2 at 620 K. Jung and Kim[13] performed solid-state reactions and hot pressing, and obtained a maximum ZT of 0.7 at 830 K for Bi-doped Mg_2Si. Shida et al.[14,15] and Tani and Kido[16] used spark plasma synthesis (SPS) and achieved a maximum ZT of 0.86 at 862 K with Bi-doped Mg_2Si. The vertical Bridgman method was used by Akasaka et al.[17] and Tamura et al.[18] for growth of single crystals of Mg_2Si. Melt-spinning followed by SPS or hot pressing was attempted by Li et al.[19] to consolidate the thermoelectric material. They demonstrated that thermoelectric properties could be enhanced by using a non-equilibrium quenching technique.

Thermal spraying is a cost-effective, flexible, and industry-scalable manufacturing process that has been widely used in the aerospace and automotive industries. In the past decade Sampath[20] extended this technique to the synthesis of functional electronics and sensor materials. Similar to melt spinning,[21] thermal spraying has a very high quenching rate (10^6–10^7 K/s).The working mechanism of atmospheric plasma spraying (APS) includes generation of plasma gas by use of a strong electric field, melting the powder by use of the high temperature plasma gas, expanding and pushing the melted droplet toward a substrate, and forming a coating by rapid quenching on the substrate. Integrated design and manufacture of thermoelectric devices directly on the exhaust system by thermal spraying was recently proposed by Zuo and co-workers.[22,23] Preliminary results for thermally sprayed Mg_2Si have been reported by Fu et al.[24] Thermal spraying has recently been used to prepare $FeSi_2$ thermoelectric materials.[25–28] However, the maximum ZT of $FeSi_2$ is approximately 0.1 which is too low for practical energy recovery. Thermal spraying of Mg_2Si is much more challenging, because Mg has very high vapor pressure and high reactivity with O_2; it has not been reported by others.

In this study, low-temperature high-velocity (LTHV) APS was used to fabricate Mg_2Si samples. The samples were characterized by measurement of thermal conductivity, electric conductivity, and Seebeck coefficient, and the results were compared with those of samples prepared from the same powder by use of the hot-pressing method. The purpose was to identify the optimum thermal spraying process conditions that achieved a phase composition similar to that of the feedstock powder. The microstructure was also compared with that of samples prepared by use of the conventional hot-pressing method. We also studied the effect of carrier concentration and mobility on the thermoelectric properties. Although the ZT of thermally sprayed samples was only 10% that of hot-pressed samples, the target application is automotive exhaust systems, which require plentiful, inexpensive materials, high-volume production, low-cost application, and reliability. Thermal spray processing has many of these benefits, and adapting it to high-volume thermoelectric device fabrication would be a major advance.

EXPERIMENTAL

Mg_2Si powder (>98%) purchased from YHL New Energy (Zhejiang, China) was used to deposit samples on $40 \times 25 \times 2$ mm^3 aluminium substrates. Measurement revealed the size of the original powder ranged from 10 μm to 270 μm. The powder was sieved from 53 μm to 180 μm for use as feedstock powder. The purity of the powder was 98%; higher purity is desirable, but is both very expensive and not readily available with the desired powder size and shape. A 40-kW plasma-spray system (Miller Thermal, USA) was used to deposit the Mg_2Si feedstock powder. As shown in Table I argon was used as the main plasma-forming gas, with helium used as the powder carrier gas. Other thermal spray process conditions are also listed in Table I.

Hot-pressed samples were fabricated by use of the same powder provided by the same company. Table II lists all the samples synthesized by use of

the thermal spraying or hot-press techniques, with annealing conditions, and the density determined by measuring mass by use of a balance with readability of 0.001 g (AV264; Ohaus, US) and volume by measuring the length, width, and height of the sample by use of calipers (Mitutoyo, US).

The sample phase was analyzed by x-ray diffraction (XRD; PAD-V; Scitag, CA, USA), utilizing CuKα radiation, and by x-ray spectroscopy (EDX; Leo-1550-SFEG; Carl Zeiss SMT, Cambridge, UK). Cross-sectional morphology of the samples was studied by scanning electron microscopy (SEM; Leo-1550-SFEG). Electrical conductivity in the temperature range 300–380 K was measured by the four-probe method by use of the physical property measurement system (PPMS; Quantum Design, CA, USA), and the Seebeck coefficient was measured by use of an MMR Seebeck S100 controller with a K20 temperature controller (MMR Technologies, CA, USA). Thermal conductivity was measured by use of the laser flash method (FS3500; TA Instrument, DE, USA). To investigate their contribution to electrical conductivity, carrier concentration and mobility were measured by use of a Hall measurement system (8404; Lake Shore Cryotronics, OH, USA).

Table I. Plasma spray conditions

Plasma gas	Argon
Carrier gas	Helium
Current (A)	450
Flow rate (SLPM)	105
Flow rate (SLPM)	34.8
Raster (mm/s)	500
Pulse (s)	2
Step (mm)	2
Powder feed rate (g/min)	5–8
Stand-off distance (mm)	100

RESULTS AND DISCUSSION

Phase Composition of Powder, and Hot-Pressed and Thermally Sprayed Samples

Figure 1 shows the XRD of the feedstock powder, and of samples made by APS and by hot pressing. The reaction temperature between Mg_2Si and O_2 is approximately 450°C, and the temperature during thermal spraying is much higher than this. To avoid significant oxidation, the APS torch was equipped with an internal powder distributor that can produce a high-velocity, low-temperature particle stream, in an attempt to suppress oxidation of Mg_2Si.

Sample A1 is the as-sprayed sample without heat treatment. The XRD results showed that the APS samples have a composition highly consistent with the feedstock powder, although small MgO and Si

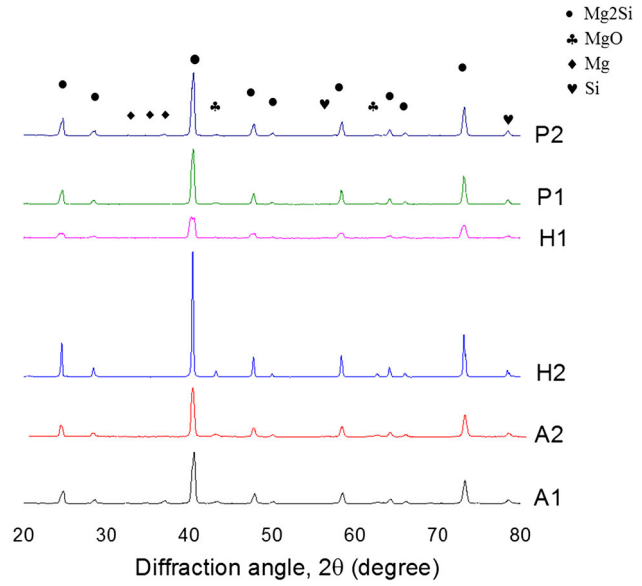

Fig. 1. XRD of powder with nominal ratio (P1) and Mg-rich (P2), as-sprayed (A1) and vacuum annealed (A2) samples, and hot pressed with nominal ratio (H1) and Mg rich (H2).

Table II. Sample synthesis conditions and powder information

Sample	Synthesis	Conditions	Annealing	Other	Density
P1	(Powder)	N/A	None	Normal ratio	N/A
P2	(Powder)	N/A	None	Mg rich	N/A
A1	APS	LTHV	None	Mg rich	79%
A2	APS	LTHV	400°C, 1 h	From A1	80%
A3	APS	LTHV	400°C, 20 h	From A1	80%
A4	APS	LTHV	750°C, 20 h	From A1	80%
H1	HP	800°C, 30 MPa	None	Normal ratio	85%
H2	HP	800°C, 30 MPa	None	Mg rich	90%

APS atmospheric plasma sprayed, *HP* hot-pressed.

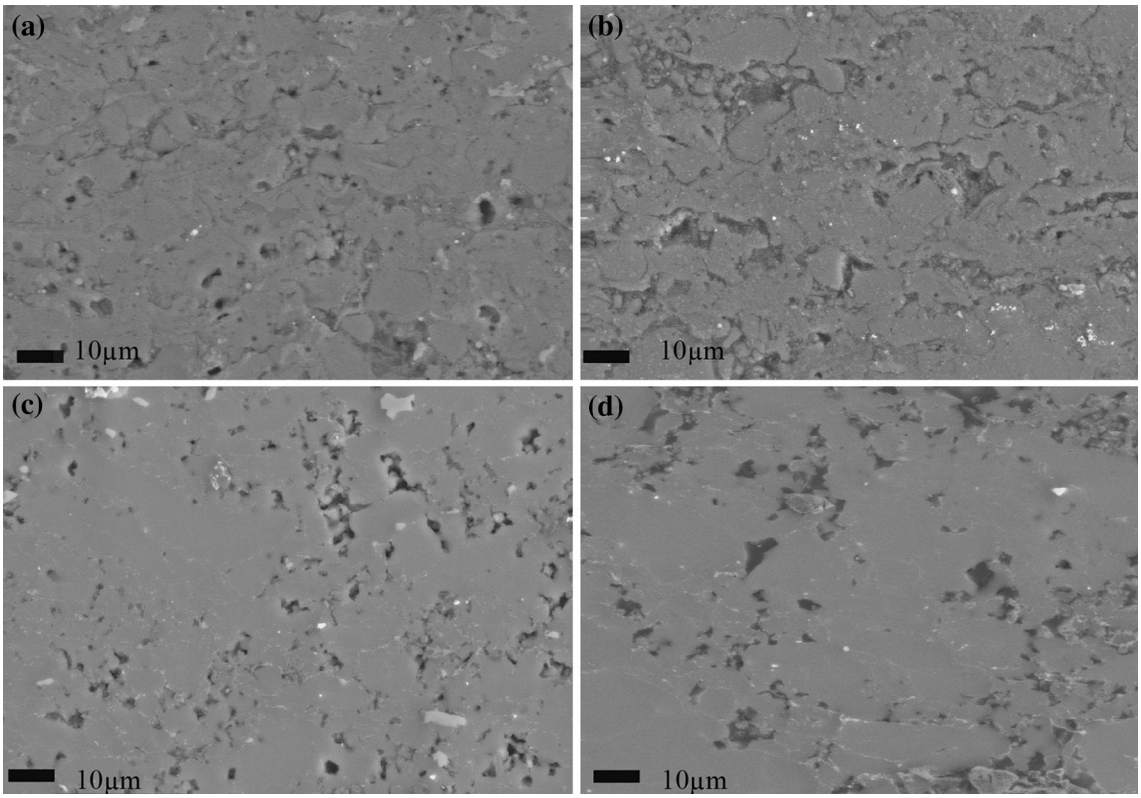

Fig. 2. SEM cross sections of APS samples A1 (a) and A2 (b) and hot-pressed samples H1 (c) and H2 (d). It is apparent that APS samples have more pores and cracks.

peaks are observed. The Mg peak found in the sample may arise from the original powder. After vacuum heat treatment APS (A2) no Mg peak was observed, possibly because of oxidation or volatilization of Mg during the heat treatment.

Fabrication of the hot-pressed sample was conducted under vacuum at a heating rate of 5°/min and with cooling rates of 3–5°/min. Hot-pressed samples using both powders furnished no clear Mg peak, however the Mg-rich powder resulted in more MgO peaks, possibly because of oxidation during vacuum hot pressing. Because XRD is limited in the smallest concentration it can resolve, small quantities of impurities may not be observed by XRD.

SEM Results for Thermally Sprayed Samples

Figure 2a, b shows cross section SEM images of APS samples A1 and A2; Fig. 2c, shows images for hot-pressed samples H1 and H2. It is apparent that the APS samples have a large number of pores and cracks compared with hot-pressed samples (H1 and H2). Heat treatment of APS sample A2 did not substantially anneal this defect, and the low heat treatment temperature of 400°C could be the reason, because it is far less than two thirds of the melting point of Mg_2Si (1100°C). The APS images also show evidence of unmelted particles, because of the low temperature and the high-velocity spray conditions. Such spray conditions tend to only soften the powder particles instead of melting them, and was used to avoid Mg_2Si oxidation during the process. SEM images of the hot-pressed samples indicate that the Mg-rich powder has a denser microstructure, probably because of the ductile–brittle properties of Mg_2Si. The hot-pressing process was performed at 30 MPa for both powders. Although the resulting samples were not fully dense, far fewer cracks and pores were found compared with the APS samples.

Thermoelectric Properties of Mg_2Si

The thermoelectric properties thermal conductivity, electrical conductivity, and Seebeck coefficient were determined and compared for APS and hot-pressed samples and with reported data.

Thermal Conductivity

Figure 3 shows the thermal conductivity of Mg_2Si prepared by APS and by hot pressing. The thermal conductivity was measured from 300 K to 390 K in a nitrogen environment. Thermally sprayed samples A1 and A2 have thermal conductivity at least 40% lower than for the hot-pressed samples. This is probably because of the large numbers of pores and cracks present in the sample,[29–31] because the more porous the sample, the less thermally conductive.

Electrons also contribute to the thermal conductivity. The reduced thermal conductivity of sample A2 is probably because of the reduced electronic contribution from the lower electron concentration, as indicated by the Hall effect measurements discussed below. Compared with sample Ref1 of Jung and Kim[13] who reported a thermal conductivity of *n*-type Mg_2Si of approximately 5.3 W/m K and sample Ref2 of Tian and Kido[16] who reported a thermal conductivity of Mg_2Si of 10.6 W/m K, our 3.6 W/m K for A1 and 2.2 W/m K for A2 shows the thermal-spray method can be used as a new technique for fabrication of thermoelectric material to improve reduction of the thermal conductivity.

Figure 4a clearly shows the electronic contribution of the thermal conductivity κ_{el} of thermally sprayed and hot-pressed sample. This electronic contribution is calculated by use of the equation $\kappa_{el} = L_0 \sigma T$, where L_0 is the Lorenz number, given as $2.45 \times 10^{-8} V^2/K^2$.[16] The electrical conductivity σ is shown in Fig. 5 below. Basically, the high electrical conductivity leads to a high electronic contribution to thermal conductivity. This indicates that after heat treatment the electrical conductivity of A2 is reduced because of the reduced electronic contribution. Figure 4b shows the phonon contribution $\kappa_{ph} = \kappa - \kappa_{el}$ and also shows the dominant part is the lattice contribution to thermal conductivity.

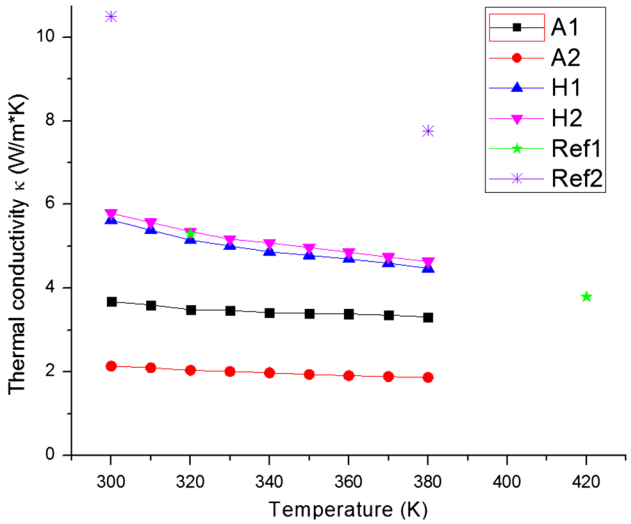

Fig. 3. Thermal conductivity of Mg_2Si prepared by APS (A1 and A2) is lower than that of Mg_2Si prepared by hot pressing (H1, H2) and in other work (Ref1, Ref2).

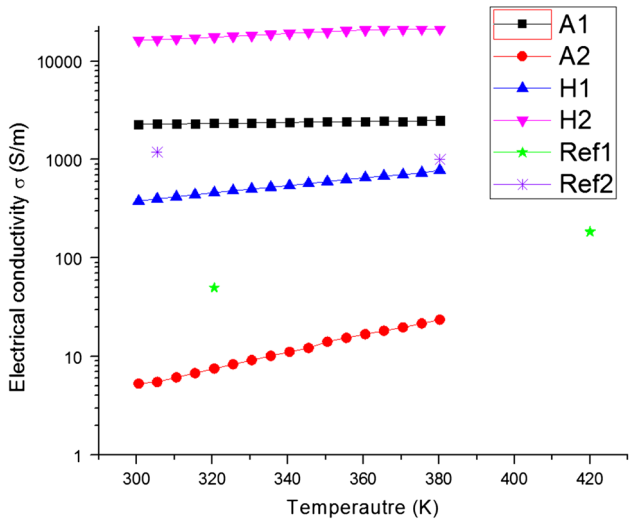

Fig. 5. The electrical conductivity of Mg_2Si by prepared APS (A1) is similar to that of with hot-pressed samples (H1 and H2), which is comparable with reported values (Ref1, Ref2).

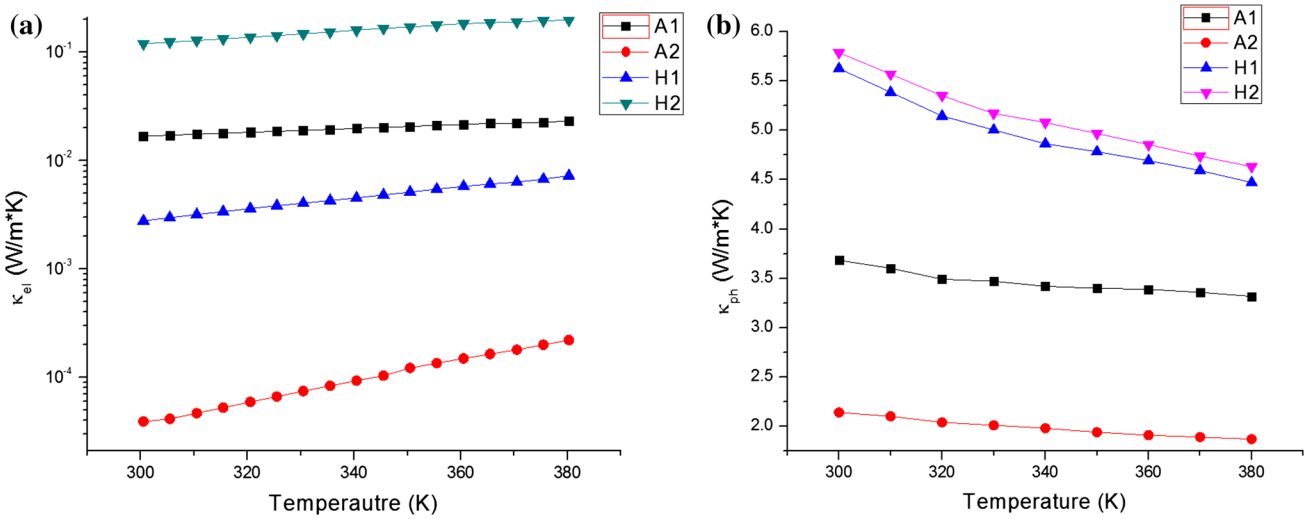

Fig. 4. Carrier contribution κ_{el} (a) and lattice contribution κ_{ph} (b) to the thermal conductivity of Mg_2Si prepared by APS (A1, A2) and hot pressing (H1, H2).

Table III. Results from Hall effect measurement of Mg_2Si prepared by APS and by hot pressing, and reported values

Sample	Carrier concentration, n (10^{17}/cm^3)	Mobility, μ (cm^2/V·s)	Conductivity, $\sigma = ne\mu$ (S/m)
A1	4,270	0.15	1,025
A2	8.3	0.51	7
A3	1.2	0.52	1
A4	1.7	4.48	12
H1	22.6	13.31	481
H2	258	26.72	11,040
Ref1	0.3	104.2	50
Ref2	4.3	204	1404

Electrical Conductivity and Hall effect Measurements

Electrical conductivity was measured from 300 K to 390 K by use of the PPMS. The measured electrical conductivity of APS samples and hot-pressed samples are shown in Fig. 5. It is apparent that variations of the electrical conductivity of the samples are significant. Ref1 and Ref2 are values reported by Jung and Kim[13] and Tani and Kido.[16] For the APS sample, A1 has much higher conductivity than A2. This is because of the much higher carrier concentration in A1, as shown in Table III. A2 was obtained from A1 by heat treatment, and during heat treatment the excess Mg in the coating is oxidized or evaporated, because Mg is very sensitive to air and has a very high vapor pressure.

Of the hot-pressed samples, H2 had higher conductivity than H1, probably because of the additional Mg present in the raw powder. To understand the mechanisms and key properties that affect electrical conductivity. Hall effect measurements were performed at room temperature; the results are shown in Table III.

The electrical conductivities $\sigma = ne\mu$ in Table III, calculated on the basis of the Hall measurements, are in good agreement with the PPMS measurements at 300 K, shown in Fig. 4. Ref1 and Ref2 are reported values from Jung and Kim[13] and Tani and Kido[16] The APS sample without heat treatment (A1) has the highest carrier concentration and A3 the lowest. The high carrier concentration in sample A1 is because of the controlled temperature and velocity of thermal spraying. By using the SG100 gun, the internal powder-distribution system can avoid oxidation of the excess Mg during spraying because the powder is injected directly into the plasma flame center instead of being injected from the outer surface the plasma flame. Also, the velocity of the thermal spray was very high, which can reduce the time of flight for the melted droplet thus reduce the oxidation time during this period. The low temperature setting further suppresses oxidation or evaporation of Mg during coating, which results in a high carrier concentration in sample A1. After heat treatment, sample A2 has a reduced carrier concentration, because the chamber is not under 100% vacuum and the excess Mg is oxidized or evaporated during the heat treatment. As a matter of fact, carrier concentration is lower for longer-heat treatment time, as is apparent from Table III. The mobility of the APS samples is also significantly lower than that of the hot-pressed samples. Generally, for semiconductor materials, mobility is determined by phonon scattering at high temperatures and ionized impurity scattering at low temperatures.[32] The samples in this study are highly disordered, with the result that the mobility is far less than for the other bulk material (i.e. the SPS method), as shown in Table III.

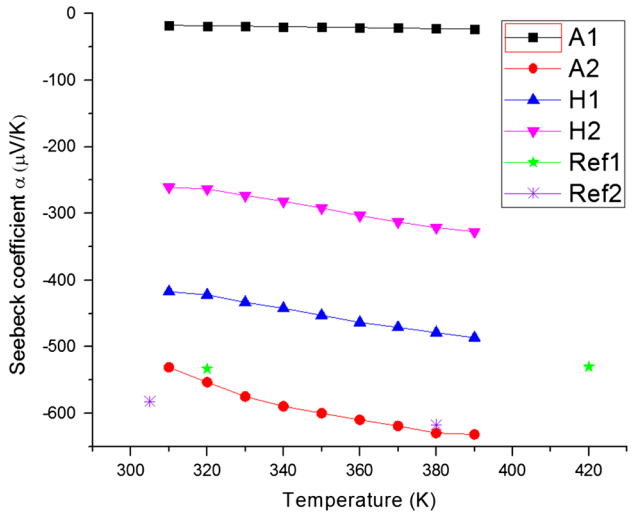

Fig. 6. The Seebeck coefficient of Mg_2Si produced by APS (A1) is increased by reducing the carrier concentration (A2). The Seebeck coefficient of Mg_2Si produced by hot pressing with nominal ratio powder (H1) is higher than for that produced with Mg-rich powder (H2).

The low mobility of the APS sample may also be because of impurities in the raw powder. During processing, magnesium will evaporate more readily than elements such as iron, nickel, and manganese, all of which were detected in the APS sample and raw powder by use of EDX. The increased impurity concentration will scatter electrons more strongly, resulting in reduced mobility. Copper was also found in the APS samples, only, most probably as a result of erosion of the copper thermal spray nozzle.

After 400°C heat treatment under vacuum, mobility is increased by a factor of approximately three, as is apparent from the mobility for samples A2 and A3. The mobility is further increased by higher-temperature heat treatment A4. This increase may be because of grain size growth. On the other hand, Mg_2Si and Mg can react with residual oxygen in the vacuum chamber during annealing, which may explain the dramatic decrease in carrier concentration for samples A2, A3, and A4. The heat treatment does help to increase the mobility but the annealing temperature is critical.

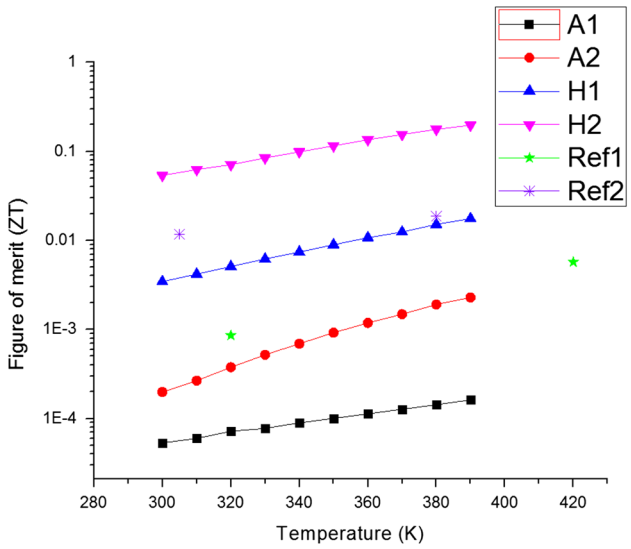

Fig. 7. *ZT* of Mg_2Si produced by APS (A1) increased after annealing (A2) and reached 10% of that of the hot-pressed sample.

Seebeck Coefficient

Figure 6 shows the measured Seebeck coefficients for the APS and hot-pressed samples. It has been reported the Seebeck coefficient is not affected by microstructure; rather it depends on phase composition.[33] The Seebeck coefficient is inversely proportional to electrical conductivity, because of the opposite dependence of carrier concentration, i.e., $S \sim \ln(1/n)$ in Eq. (2).[8] Figure 6 and Table 3 indicate that the Seebeck coefficient decreases with increased carrier concentration. The negative Seebeck coefficient indicates that un-doped Mg_2Si is an *n*-type semiconductor.[16] The Seebeck coefficient of as-sprayed sample A1 is very low, because the carrier concentration is too high. During heat treatment some of the Mg was vaporized or oxidized, and thus sample A2 has a lower carrier concentration and a dramatically increased Seebeck coefficient.

For the hot-pressed samples, the Mg-rich sample H2 had a lower Seebeck coefficient because of its higher carrier concentration, with all other properties being similar to those of H1. The hot-pressed samples had carrier concentrations between those of APS samples A1 and A2, and the Seebeck coefficients were similarly situated between the values for samples A1 and A2. In comparison with the Seebeck coefficient of 530 μV/K for the heat treated A2 sample, that for Ref1 by Jung and Kim[13] was 550 μV/K and that for Ref2 by Tani and Kido[16] was 590 μV/K. This showed the thermally sprayed sample after heat treatment had a Seebeck coefficient comparable with reported values.

Figure of Merit

Figure 7 shows the figure of merit *ZT* (Eq. 1) for the APS and hot-pressed samples, with reported data. Ref1 and Ref2 are values reported by Jung and Kim[13] and Tani and Kido.[16] The APS samples have a lower *ZT* than the hot-pressed samples, even though the APS samples have much lower thermal conductivity. This reduction occurs primarily because the as-sprayed sample has a very low Seebeck coefficient whereas the annealed sample has very low electrical conductivity.

For APS, vacuum-annealed sample A2 had a higher *ZT* than the as-sprayed sample A1. Although A1 has much higher electrical conductivity than A2, the Seebeck coefficient of A1 is nearly 25 times less than that of A2. Also, the thermal conductivity of A2 is only approximately half that of A1, which results in a higher *ZT* for A2.

For the hot-pressed samples, nominal-ratio powder sample H1 had a lower *ZT* than the Mg-rich sample H2. H2 has much higher electrical conductivity than H1, and, noting their similar Seebeck coefficient and thermal conductivity, H2 has a higher *ZT* than H1. Heat treatment of the APS material can increase the figure of merit, and it should be possible to increase it further by appropriate doping. Annealing at higher temperature further increases the mobility, and appropriate doping can be used to adjust the carrier concentration to the optimum for maximizing the thermoelectric properties of APS samples.

CONCLUSIONS

Magnesium silicide (Mg_2Si) deposits have been synthesized by APS, which has been shown to be an effective way of reducing the thermal conductivity of material compared with the conventional hot-press method. Although Mg_2Si is very sensitive to oxidation and temperature, the APS approach, using an internal powder distributor system, successfully maintains the composition of the deposit similar to that of the starting powder. In this work, the reduced thermal conductivity of the Mg_2Si material is most likely to be because of increased pores and cracks in the APS samples. Thermal conductivity, electrical conductivity, Seebeck coefficient, and figure of merit were all compared for APS and hot-pressed samples for temperatures ranging from 300 K to 390 K. Carrier concentration and Hall mobility were measured to assess their relative contribution to the electrical conductivity. Reported values of the thermoelectric properties were also compared with our experimental data. Carrier concentration is a compromise between electrical conductivity and Seebeck coefficient. Heat treatment under vacuum at 400°C improves the carrier concentration but does not change the mobility as significantly as at 750°C. The Seebeck coefficient increases with decreasing carrier concentration if the phase remains the same. The thermal conductivity of APS samples is lower than that of hot-pressed samples, primarily as a result of geometric effects because of the large number of pores and cracks in the coating. Vacuum-annealed APS samples have a very high Seebeck coefficient.

Carrier concentration must be adjusted and carrier mobility must be increased to further improve *ZT*. Although the *ZT* of thermally sprayed samples was only 10% that of hot-pressed samples, the target application is automotive exhaust systems, which require plentiful, inexpensive materials, high-volume production, low-cost application, and reliability. Thermal spray processing already has many of these benefits, and adapting it to high-volume thermoelectric device fabrication would be a major advance. Further improvement of *ZT* of APS samples is expected to be achieved by appropriate control of the carrier concentration combined with high temperature annealing. This work suggests that thermal spraying may be a viable means of direct fabrication of thermoelectric materials for high-volume applications.

ACKNOWLEDGEMENTS

The authors gratefully acknowledge financial support from the NSF/DOE Thermoelectrics Partnership program under grant NSF CBET #1048744 and from NYSERDA under Contract 21180. The authors wish to thank Dr Jim Quinn, Dr Xiaoya Shi, Mr Bo Zhang, and Ms Su Jung Han from Stony Brook and Dr Ming Lu and Fernando Camino from Brookhaven National Laboratory, for help in characterizing the Mg_2Si samples. We also thank Professor Richard Gambino for insightful discussions and Professor Fuxing Ye for assistance with hot pressing.

REFERENCES

1. S.C. Davis and S.W. Diegel, *Transportation Energy Data Book* (Oak Ridge, Tenn: Oak Ridge National Laboratory, 2012).
2. J.H. Yang and F.R. Stabler, *J. Electron. Mater.* 38, 1245 (2009).
3. D.H. Wei, X.S. Lu, Z. Lu, and J.M. Gu, *Energy Convers. Manag.* 48, 1113 (2007).
4. N. Ishikawa, *Int. J. Engine Res.* 13, 99 (2012).
5. T. Katrasnik, S. Rodman, F. Trenc, A. Hribernik, and V. Medica, *J. Eng. Gas Turbines Power Trans. Asme* 125, 590 (2003).
6. P. Patel, *MIT Technology Review* (2011).
7. G. Min, D.M. Rowe, and K. Kontostavlakis, *J. Phys. D* 37, 1301 (2004).
8. G. Busch and U. Winkler, *Helv. Phys. Acta* 26, 395 (1953).
9. R.G. Morris, R.D. Redin, and G.C. Danielson, *Phys. Rev.* 109, 1909 (1958).
10. R.J. Labotz, D.R. Mason, and D.F. Okane, *J. Electrochem. Soc.* 110, 127 (1963).
11. V.K. Zaitsev, M.I. Fedorov, E.A. Gurieva, I.S. Eremin, P.P. Konstantinov, A.Y. Samunin, and M.V. Vedernikov, *Phys. Rev. B* 74, 045207 (2006).
12. Y. Isoda, S. Tada, T. Nagai, H. Fujiu, and Y. Shinohara, *Mater. Trans.* 51, 868 (2010).
13. J.Y. Jung and I.H. Kim, *Electron. Mater. Lett.* 6, 187 (2010).
14. K.S. Shida, K. Shiraishi, T. Ito, M. Omori, and T. Hirai, *Thermoelectric figure of merit of impurity doped and hot-pressed magnesium silicide elements*, 1998.
15. K.S. Shida, S. Suhihara, M. Ohmori, and T. Hirai, *Thermoelectric properties of magnesium silicide processed by powdered elements plasma activated sintering method*, 1997.
16. J. Tani and H. Kido, *Physica B Condens. Matter.* 364, 218 (2005).
17. M. Akasaka, T. Iida, T. Nemoto, J. Soga, J. Sato, K. Makino, M. Fukano, and Y. Takanashi, *J. Cryst. Growth* 304, 196 (2007).
18. D. Tamura, R. Nagai, K. Sugimoto, H. Udono, I. Kikuma, H. Tajima, and I.J. Ohsugi, *Thin Solid Films* 515, 8272 (2007).
19. Q. Li, Z.W. Lin, and J. Zhou, *J. Electron. Mater.* 38, 1268 (2009).
20. S. Sampath, *J. Therm. Spray Technol.* 19, 921 (2010).
21. J. Zhou, Q. Jie, L.J. Wu, I. Dimitrov, Q. Li, and X. Shi, *J. Mater. Res.* 26, 1842 (2011).
22. J.P. Longtin, L. Zuo, D. Hwang, G.S. Fu, M. Tewolde, Y.K. Chen, and S. Sampath, *J. Therm. Spray Technol.* 22, 577 (2013).
23. L. Zuo, J.P. Longtin, S. Sampath, Q. Li, and B. Li, DOE, *Thermoelectrics Workshop* (2011).
24. G. Fu, L. Zuo, J.P. Longtin, C. Nie, Y.K. Chen, M. Tewolde, and S. Sampath, *Fall MRS at Boston* (2012).
25. M. Cherigui, N.E. Fenineche, and C. Coddet, *Surf. Coat. Technol.* 192, 19 (2005).
26. J. Schilz, E. Muller, K. Schackenberg, H. Ernst, W.A. Kaysser, G. Langer, and E. Lugscheider, *J Mater. Sci. Lett.* 17, 1487 (1998).
27. Y.T. Makita, H. Takahashi, H. Shibata, N. Kobayashi, M. Hasegawa, S. Kimura, A. Obara, J. Tanabe, and S. Uekusa, *Optical, electrical and structural properties of polycrystallinel beta-$FeSi_2$ thin films fabricated by electron beam evaporation of ferrosilicon*, 1996.
28. S.S. Sodeoka, M. Suzuki, A. Tsutsumi, K. Kuramoto, J. Sawazaki, K. Yoshida, H. Huang, K. Nagai, H. Kondo, and S. Nakahama, *Fabrication of large size $FeSi_2$ thermoelectric device by thermal spraying process*, 1998.
29. W.G. Chi, S. Sampath, and H. Wang, *J. Am. Ceram. Soc.* 91, 2636 (2008).
30. N.P. Padture, M. Gell, and E.H. Jordan, *Science* 296, 280 (2002).
31. L. Pawlowski, *The science and engineering of thermal spray coatings* (2008).
32. N.D.H. Arora, J.R. Hauser, and D.J. Roulston, *IEEE Trans. Electron. Devices* 29, 292 (1982).
33. Y.F. Hu, E. Sutter, W.D. Si, and Q. Li, *Appl Phys Lett* 87, 171912 (2005).